

## Structural reinforcement of cell-laden hydrogels with microfabricated three dimensional scaffolds†

Cite this: *Biomater. Sci.*, 2014, **2**, 703

Chaenyung Cha,<sup>a,b</sup> Pranav Soman,<sup>c,e</sup> Wei Zhu,<sup>c</sup> Mehdi Nikkhah,<sup>a,b</sup> Gulden Camci-Unal,<sup>a,b</sup> Shaochen Chen<sup>\*c</sup> and Ali Khademhosseini<sup>\*a,b,d</sup>

Hydrogels commonly used in tissue engineering are mechanically soft and thus often display structural weakness. Herein, we introduce a strategy for enhancing the structural integrity and fracture toughness of cell-laden hydrogels by incorporating a three-dimensional (3D) microfabricated scaffold as a structural element. Digital micromirror device projection printing (DMD-PP) system, a rapid prototyping technology which employs a layer-by-layer stereolithographic approach, was utilized to efficiently fabricate 3D scaffolds made from photocrosslinkable poly(ethylene glycol) diacrylate (PEGDA). The scaffold was incorporated into a photocrosslinkable gelatin hydrogel by placing it in a pre-gel solution, and inducing *in situ* hydrogel formation. The resulting scaffold-reinforced hydrogels demonstrated a significant increase in ultimate stress and provided structural support for mechanically weak hydrogels. In addition, the scaffold did not affect the rigidity of hydrogels, as it was not involved in the crosslinking reaction to form the hydrogel. Therefore, the presented approach could avoid inadvertent and undesired changes in the hydrogel rigidity which is a known regulator of cellular activities. Furthermore, the biocompatibility of scaffold-reinforced hydrogels was confirmed by evaluating the viability and proliferation of encapsulated fibroblasts. Overall, the strategy of incorporating 3D scaffolds into hydrogels as structural reinforcements presented in this study will be highly useful for enhancing the mechanical toughness of hydrogels for various tissue engineering applications.

Received 9th September 2013,  
Accepted 14th October 2013

DOI: 10.1039/c3bm60210a

www.rsc.org/biomaterialsscience

### 1. Introduction

Hydrogels are widely used as scaffold materials for tissue engineering applications, because their structure, a crosslinked network of polymers with high fluid content and elasticity, closely mimics native extracellular matrices (ECM) and therefore provides a suitable microenvironment for cells and tissues.<sup>1–4</sup> Various strategies have been employed to control the biochemical and mechanical properties of the hydrogels. For example, ECM proteins (*e.g.* collagen, laminin and fibronectin)<sup>5–7</sup> or their

functional peptide sequences (*e.g.* RGD peptide)<sup>8–10</sup> are chemically incorporated into hydrogels to induce cell adhesion to the hydrogel surface. The rigidity of hydrogels is often modulated by controlling the crosslinking density.<sup>11,12</sup>

In order to emulate the natural biomechanical environment of the cells, the hydrogel rigidity is often controlled to match the inherent softness of native ECM.<sup>13–15</sup> However, due to the structural weakness of hydrogels, they are easily broken and often display a high degree of swelling. As a result, handling hydrogels becomes challenging, and their original structure and dimensions often do not remain intact over time. There are various reinforcement strategies to improve the toughness of the hydrogels. For example, a secondary polymeric network is introduced to strengthen the hydrogels (*e.g.* formation of interpenetrating networks).<sup>16,17</sup> In addition, nanostructures are incorporated into the polymeric network to create composite hydrogels (*e.g.* clay, minerals, polymeric and metal nanospheres).<sup>18,19</sup> However, these approaches often result in changes in rigidity and diffusion properties of hydrogels, which influence the cellular phenotypes.<sup>20,21</sup> Similarly, it has been shown that nanostructures could elicit non-specific responses from cells.<sup>22</sup> Therefore, it is desirable to employ a strategy that only enhances the structural integrity and fracture resistance of hydrogels without inadvertently influencing their cell responsiveness.

<sup>a</sup>Division of Biomedical Engineering, Department of Medicine, Brigham and Women's Hospital, Harvard Medical School, Cambridge, MA 02139, USA.

E-mail: alik@rics.bwh.harvard.edu; Fax: +1-617-768-8202; Tel: +1-617-388-9271

<sup>b</sup>Harvard-MIT Division of Health Sciences and Technology, Massachusetts Institute of Technology, Cambridge, MA 02139, USA

<sup>c</sup>Department of Nanoengineering, University of California, San Diego, La Jolla, CA 92093, USA. E-mail: chen168@eng.ucsd.edu; Fax: +1-858-534-9553;

Tel: +1-858-822-7856

<sup>d</sup>Wyss Institute for Biologically Inspired Engineering, Harvard University, Boston, MA 02115, USA

<sup>e</sup>Department of Biomedical and Chemical Engineering, Syracuse University, Syracuse, NY 13244, USA

†Electronic supplementary information (ESI) available: Supporting figures associated with this article are available in ESI. See DOI: 10.1039/c3bm60210a

Here, we present an approach to enhance the structural integrity and toughness of hydrogels by introducing a 3D polymeric scaffold designed to act as a structural framework to reinforce the hydrogels. This approach was inspired by the endoskeletal system of vertebrate species, which has evolved not only to provide structural support and protection for tissue structures, but also to guide their overall shape.<sup>23</sup> Therefore, we hypothesized that the presence of a solid scaffold would support the structural integrity and increase the fracture strength of soft cell-laden hydrogels without affecting their rigidity. The scaffold made of poly(ethylene glycol)diacrylate (PEGDA) was developed by digital micromirror device projection printing (DMD-PP), a rapid prototyping stereolithography technique which allows for a highly efficient fabrication of three dimensional (3D) structures in micro-scale dimensions.<sup>24–27</sup> The concentration of PEGDA was varied to control the flexibility of the scaffolds. Then, the scaffold was immersed in a pre-gel solution containing methacrylated gelatin (GelMA) and a photoinitiator, followed by UV irradiation to fabricate the scaffold-reinforced hydrogels. The mechanical properties of the scaffold-reinforced GelMA hydrogels were evaluated by measuring elastic moduli and ultimate stress, and were compared with those of pure GelMA hydrogels to evaluate the reinforcing effect of the PEGDA scaffold. Furthermore, fibroblasts were encapsulated within the scaffold-reinforced hydrogels and their viability and proliferation were evaluated to assess the effect of scaffolds on the cellular viability and proliferation.

## 2. Experimental section

### 2.1. Synthesis of methacrylated gelatin (GelMA)

Gelatin (10 g, Sigma Aldrich) and 4-dimethylaminopyridine (0.5 g, Sigma Aldrich) were dissolved in dimethyl sulfoxide (90 mL, Fisher) at 50 °C. Then, glycidyl methacrylate (4 mL, Sigma Aldrich) was slowly added to the solution, and the mixture was continuously stirred at 50 °C for 48 hours under dry N<sub>2</sub>. The mixture was dialyzed against deionized (DI) water, and lyophilized to obtain the product. The chemical conjugation of methacrylate to gelatin was confirmed by <sup>1</sup>H-NMR (ESI Fig. 1†).

### 2.2. Fabrication of PEGDA scaffolds with digital micromirror device projection printing (DMD-PP)

The schematic diagram of the DMD-PP system is shown in Fig. 1a. The system consists of five major components: a computer-based control system, a DMD chip (Texas Instruments), a UV light source (Green Spot, UV Source, Inc.), a projection lens assembly, and a sample stage.<sup>24,28</sup> UV light was guided through a liquid-filled fiber optic cable (6.35 mm), which converged *via* two bi-convex lenses (18 mm in diameter, 40 mm in focal length, 5 mm in spacing between lenses, Edmund Optics) to the DMD chip. The projection lens assembly, which focuses the UV light to the sample stage, consisted of two equal plano-convex lenses (25 mm in diameter, 25 mm in focal length, Edmund Optics). The aperture was placed between the

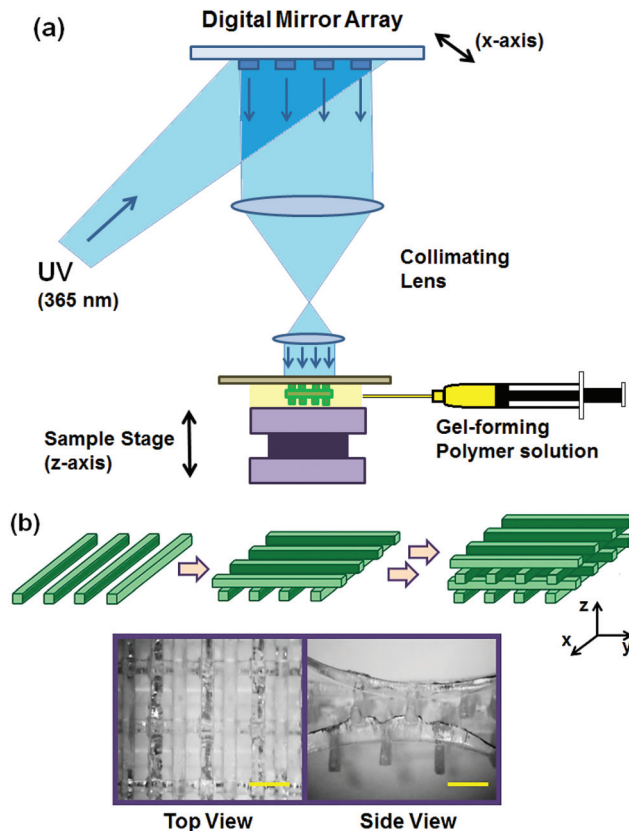


**Fig. 1** (a) Schematics of the digital mirror device projection printing (DMD-PP) system used to fabricate three dimensional (3D) PEGDA scaffolds. (b) The 3D scaffold was made *via* a layer-by-layer approach to assemble multiple scaffold layers. Each layer consisted of evenly spaced parallel bars. The photographs show top and side views of the scaffold (scale bar: 1 mm).

two lenses. All lenses used in this experiment were made from UV grade fused silica (Edmund Optics). The intensity of UV light on the sample stage was 2 mW cm<sup>-2</sup>.

The DMD chip consists of an array of 442 000 (1920 × 1080) reflective aluminum micromirrors, which can be tilted to either -10° or +10° angles with respect to the surface, which act as an “on” or “off” switch; only the light reflected off the +10° micromirror goes into the projection lens and to the sample stage, and is therefore used to fabricate the scaffold (“on”), and the light reflected off the -10° micromirror is collected by a light absorber (“off”) (ESI Fig. 2†).

The pattern of each layer of the scaffold was programmed into the DMD chip. The UV light reflected off the defined pattern of the DMD chip went through the projection lens assembly and onto the sample stage which was loaded with a pre-gel solution consisting of varying concentrations of PEGDA (20–100 wt%, *M<sub>w</sub>* 700) and Irgacure®2959 (0.5 wt%). The sample stage was adjusted vertically on a micrometer scale to determine the height of each layer. Only the UV-irradiated area was polymerized under one exposure, while the unexposed area remained in the liquid phase. After fabricating one layer, the stage was lowered and a fresh pre-gel solution was placed,

followed by UV exposure to fabricate the next layer on top of the previous one. These steps were repeated sequentially to develop the desired 3D scaffold.

### 2.3. Fabrication of scaffold-reinforced hydrogels

The scaffold was first placed in a custom-made mold made from PDMS elastomer (Sylgard® 184, Dow Corning). The pre-gel solution containing GelMA (5–10 wt%) and Irgacure® 2959 (0.1 wt%) was placed in the mold. The solution readily penetrated into the scaffold, and covered the entire mold. Then, UV irradiation was applied to induce polymerization to form hydrogels (2 minutes, output power of  $4.8 \text{ mW cm}^{-2}$ , Omni-Cure® S2000) (ESI Fig. 3†). The resulting scaffold-reinforced hydrogel was taken out of the mold, and placed in phosphate buffered saline (PBS, pH 7.4) for further characterization. The overall dimensions of the scaffold-reinforced hydrogels were  $8 \text{ mm} \times 8 \text{ mm} \times 2.5 \text{ mm}$ . The GelMA hydrogel without the scaffold was also fabricated as a control.

Scanning electron microscopy (SEM) was used to characterize the detailed morphology of the scaffold-reinforced hydrogels. A sample was frozen in liquid nitrogen, and fractured to expose the cross-section. Then the sample was dried *via* lyophilization, sputter-coated with gold (2 nm thickness, IBS/TM200S, VCR Group, Inc.), and visualized under a SEM (Quanta 200 FEG, FEI™) under high vacuum.

### 2.4. Evaluation of mechanical properties

The mechanical properties of the scaffolds, hydrogels, and scaffold-reinforced hydrogels were evaluated by measuring stress–strain curves *via* uniaxial compression at the rate of  $1 \text{ mm min}^{-1}$  until they were completely fractured, using a mechanical testing system (Model 5943, Instron®).<sup>12,29</sup> The elastic modulus of each sample was calculated from the slope of a stress–strain curve at the first 10% strain where the curve was linear. Ultimate stress was determined as the maximum stress before the scaffold-reinforced hydrogel became fractured.

Cyclic uniaxial compression tests were performed on the PEGDA scaffolds to further characterize their mechanical strengths. Briefly, each scaffold was compressed ('loading') and decompressed ('unloading') at the rate of  $1 \text{ mm min}^{-1}$  for 5 times continuously, and the stress–strain curve for both loading and unloading was recorded (Model 5943, Instron®).

### 2.5. Cell studies

NIH-3T3 fibroblasts were suspended in the pre-gel solution (cell density:  $2 \times 10^6$  cells per mL). Then, the scaffold-reinforced hydrogel was prepared as described above to encapsulate the cells. The constructs were incubated in the cell-culture media (Dulbecco's modified Eagle medium supplemented with 10% fetal bovine serum and 1% penicillin/streptomycin, all purchased from Invitrogen) at  $37^\circ \text{C}$  with 5%  $\text{CO}_2$  throughout the culture period.

To determine the viability of encapsulated cells, each sample was taken at a designated time point and the cells were fluorescently labeled with calcein-AM and ethidium homodimer-1 to identify live (green fluorescence) and dead

(red fluorescence) cells, respectively (LIVE/DEAD® Viability/Cytotoxicity Assay kit, Invitrogen), and then visualized using a fluorescence microscope (Eclipse Ti, Nikon). The viability was reported as the percentage of live cells from the total number of cells. To evaluate the actin cytoskeleton organization of cells within the hydrogel constructs, the cells were stained with Alexa Fluor®488-phalloidin (Invitrogen) and visualized using the fluorescence microscope.

## 3. Results and discussion

### 3.1. Microfabrication of PEGDA scaffolds

DMD-PP was used to fabricate 3D scaffolds which would be used as the structural framework for hydrogels (Fig. 1a). This rapid prototyping stereolithographic method utilizes a DMD chip which allows for the fabrication of micropatterned scaffolds by controlling the photocrosslinkable area with switchable micromirrors (ESI Fig. 2†). Each UV exposure reflected from the DMD chip to a gel-forming solution results in a single layer of scaffold. This photocrosslinking step was repeated on top of the previous layer to ultimately fabricate a multi-layered 3D scaffold. By controlling the DMD chip to adjust the photocrosslinked area, the architecture of the scaffold could be easily controlled on a micrometer scale. Herein, the scaffold made of photocrosslinked PEGDA consisted of four layers, each consisting of evenly spaced (1 mm) parallel bars having  $200 \mu\text{m}$  width,  $400 \mu\text{m}$  height, and 7 mm length (Fig. 1b). Each layer was aligned perpendicular to the previous one, so the inner space of the scaffold was connected throughout the structure; this ensures that the pre-gel solution can penetrate into the entire scaffold.

The concentration of PEGDA was varied from 20 wt% to 100 wt%, and then the mechanical properties of the resulting scaffolds were evaluated by uniaxial compression in the z-direction (Fig. 2a). The stress–strain curves obtained from

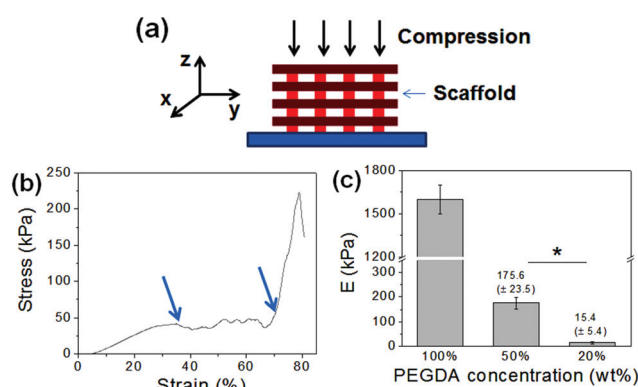


**Fig. 2** (a) Mechanical properties of PEGDA scaffolds were obtained *via* uniaxial compression. (b) A stress–strain curve of the PEGDA scaffold (100 wt%). Multiple break points within the curve (identified with arrows) are due to the gradual and partial fracture of the scaffold during the compression. (c) Elastic moduli ( $E$ ) of the PEGDA scaffolds made with varying concentrations of PEGDA (\* $p < 0.05$ ).

the uniaxial compression showed several breaks with increasing strain, due to gradual and partial breakage of the scaffolds (Fig. 2b, ESI Fig. 4†). Elastic modulus, which was determined from the slope of the initial linear region of the stress–strain curve, could be controlled in a wide range from 15.5 kPa to 1.6 MPa, demonstrating that the rigidity of the scaffold could be conveniently controlled by concentration of gel-forming polymers (Fig. 2c). Similar stress–strain profiles were obtained when the scaffolds were compressed in the *y*-direction (ESI Fig. 5†). However, the ultimate stress values for more flexible 50 wt% and 20 wt% PEGDA scaffolds were higher than those obtained in the *z*-direction, likely due to the enhanced ability of the scaffold to bend along the longer axis (*y*-direction) than the shorter axis (*z*-direction).

The mechanical strengths of the PEGDA scaffolds were further characterized by cyclic uniaxial compression (Fig. 3). The scaffolds were subjected to continuous loading and unloading for 5 cycles, and their stress–strain curves were obtained. There were no significant losses in stress values when they were repeatedly compressed below the initial break strain (<15%, Fig. 3a–c (left)). Even when they were compressed beyond their initial break strain, there were only small decreases in stress values (Fig. 3a–c (right)). These results further demonstrated their mechanical strengths and their efficacy as structural elements to reinforce soft hydrogels.

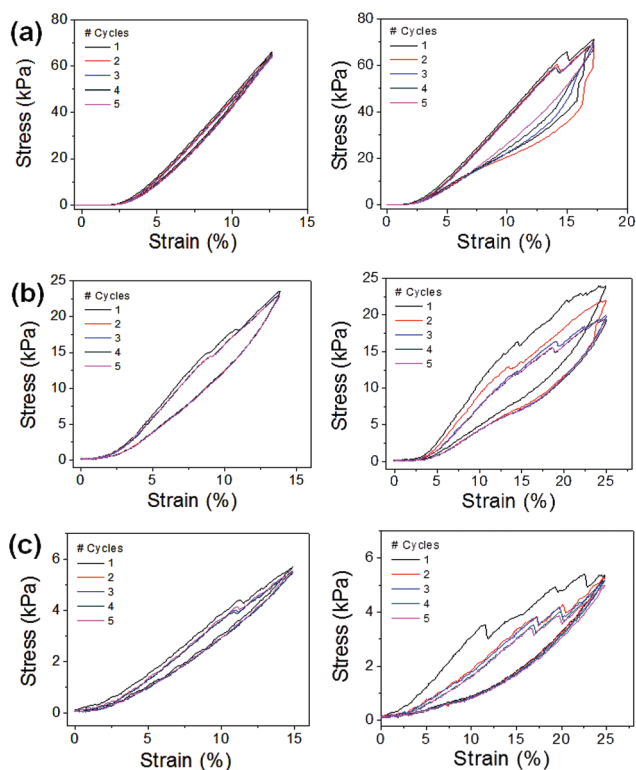


**Fig. 3** Stress–strain curves of (a) 100 wt%, (b) 50 wt% and (c) 20 wt% PEGDA scaffolds were obtained *via* cyclic compression (5 cycles). Cyclic tests were done either below (left graphs) or past (right graphs) the initial break strain.

### 3.2. Fabrication of scaffold-reinforced hydrogels

The PEGDA scaffold developed *via* DMD-PP, as described above, was used as a structural framework to improve the mechanical strength of hydrogels. For this study, GelMA was used as a model hydrogel system which has been successfully used in several applications.<sup>30–34</sup> First, the PEGDA scaffold was placed in a mold, followed by the addition of a pre-gel solution (Fig. 4a, ESI Fig. 3†). The solution quickly spread throughout the scaffold, indicating that the spacing within the scaffold was wide enough that the pre-gel solution overcame its surface tension and readily penetrated into the scaffold (ESI Fig. 6†).<sup>35,36</sup> It was also likely facilitated by the hydrophilic nature of PEGDA; the solution could spread more readily through a highly wettable surface of PEGDA scaffolds. The GelMA pre-gel solution placed in the scaffold was then irradiated with UV to fabricate the scaffold-reinforced hydrogel.

To demonstrate whether the scaffold could provide structural support for weak hydrogels, 5 wt% GelMA was used to fabricate the hydrogels, which displayed weak structural integrity and strength (Fig. 4b (left)). However, when the scaffold was introduced into these GelMA hydrogels, the original structure was well maintained (Fig. 4b (right)).

SEM was used to characterize the detailed morphology of scaffold-reinforced hydrogels. The cross-sectional SEM image showed that the GelMA hydrogel was present throughout the inner space of the scaffold, and there was no significant gap between the scaffold and GelMA hydrogels (Fig. 4c). This observation further confirmed that the pre-gel solution penetrated well into the scaffold, and the scaffold did not hinder the photocrosslinking reaction to form the GelMA hydrogel.

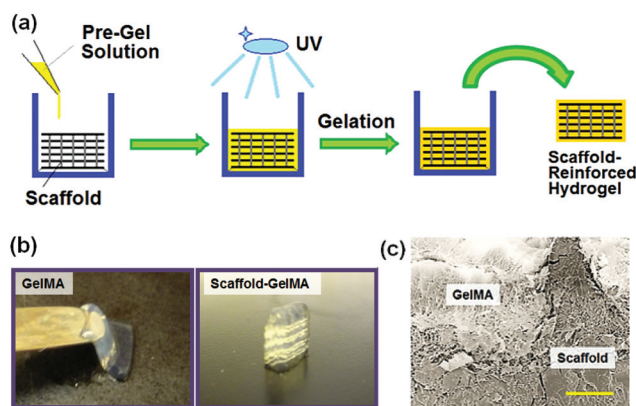


**Fig. 4** (a) Schematics of the process to fabricate scaffold-reinforced hydrogels. The microfabricated PEGDA scaffold was placed in a mold, and the pre-gel solution containing GelMA and a photoinitiator was added. Subsequent UV-initiated polymerization led to scaffold-reinforced hydrogel formation. (b) GelMA hydrogels at 5 wt% had a weak structural integrity whereas the structural integrity of the scaffold-reinforced GelMA hydrogel at the same concentration was well maintained. (c) SEM image of a cross-section of scaffold-reinforced GelMA hydrogels (scale bar: 200 μm).

### 3.3. Mechanical properties of scaffold-reinforced hydrogels

The rigidity and toughness of the scaffold-reinforced GelMA hydrogels were evaluated by measuring the elastic modulus, ultimate strain, and ultimate stress from uniaxial compression to investigate the effect of the scaffolds on the mechanical properties of the hydrogels. First, the rigidity of the PEGDA scaffolds was kept constant by using those made from 100 wt% PEGDA, and varying concentrations of GelMA, from 5 wt% to 10 wt%, were used to fabricate the scaffold-reinforced GelMA hydrogels (Fig. 5a, ESI Fig. 7†). As expected, the ultimate stress values of the GelMA hydrogels were significantly increased by the incorporation of the scaffolds, since the scaffolds acted as structural supports to protect the hydrogels from fracture (Fig. 5b). Interestingly, there was a greater increase in ultimate strain with increasing concentration of GelMA hydrogels (Fig. 5c). It is suggested that a greater mechanical strength of GelMA hydrogels at higher concentrations likely contributed to the mechanical strength of the overall scaffold-reinforced hydrogel. Elastic moduli of the GelMA hydrogels, on the other hand, were not affected by the presence of scaffolds regardless of GelMA concentrations, because the scaffolds were not involved in the crosslinking reaction of the GelMA hydrogel (Fig. 5d). These findings highlight the advantage of using a microfabricated scaffold as a structural framework, as it can significantly improve the mechanical strength of the hydrogels without altering their rigidity which is a known regulator of various cellular functions.<sup>14,15</sup> Conventional strategies to improve the mechanical strength of hydrogels, such as controlling the crosslinking density and creating composite systems, also significantly affect the rigidity of hydrogels.

We further explored the effect of the PEGDA scaffold on the mechanical properties of GelMA hydrogels by varying the rigid-

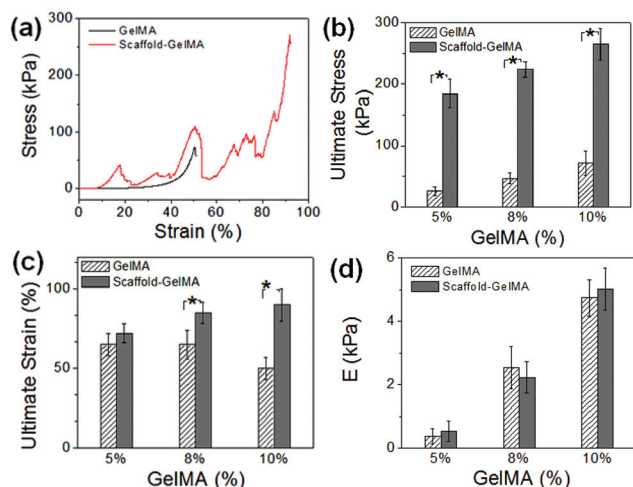


**Fig. 5** (a) Stress–strain curves of GelMA (10 wt%) and scaffold-reinforced GelMA hydrogels (scaffold-GelMA hydrogels) obtained from uniaxial compression. The microfabricated scaffold was made from 100 wt% PEGDA. (b) Ultimate stress, (c) ultimate strain and (d) elastic moduli ( $E$ ) values of GelMA hydrogels and scaffold-GelMA hydrogels. The concentration of GelMA was varied from 5 wt% to 10 wt% ( $*p < 0.05$ ).

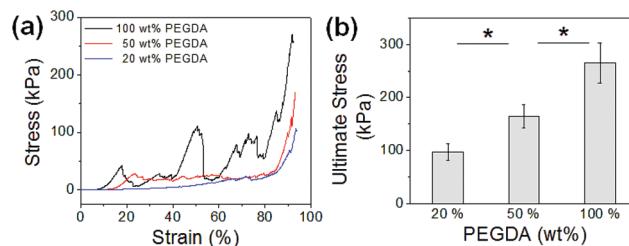


**Fig. 6** (a) Stress–strain curves of GelMA hydrogels (10 wt%) reinforced with PEGDA scaffolds with varying rigidity. The scaffolds were made by varying the concentration of PEGDA (20, 50 and 100 wt%). (b) Ultimate stress values of scaffold-GelMA hydrogels with varying the scaffold rigidity ( $*p < 0.05$ ).

ity of the PEGDA scaffolds (Fig. 6a). The concentration of GelMA hydrogels was 10 wt%, and scaffolds made from varying concentrations of PEGDA (20, 50, and 100 wt%), as shown in Fig. 2, were used to reinforce the hydrogels. As expected, elastic moduli of the GelMA hydrogels were not affected by the rigidity of the scaffolds. On the other hand, their ultimate stress increased with the rigidity of the scaffolds (Fig. 6b), which further proves that the rigidity of the scaffold directly affects the mechanical strength of the overall scaffold-hydrogel constructs.

### 3.4. Cell encapsulation in scaffold-reinforced hydrogels

To evaluate the effect of scaffold reinforcement on the biocompatibility of cell-laden hydrogels, NIH-3T3 fibroblasts were encapsulated within GelMA hydrogels and GelMA hydrogels reinforced with PEGDA scaffolds. The concentration of GelMA hydrogels was 8 wt%, and the scaffold made from 100 wt% PEGDA was used to reinforce the GelMA hydrogels. The viability of fibroblasts in GelMA, regardless of the presence of the scaffold, was well maintained (>80%) throughout the culture period (Fig. 7a and b). The cells within the hydrogels began to spread after 3 days of culture and proliferated within the hydrogel over time. After 3 weeks of culture, the cells proliferated extensively and covered the entire hydrogel area, resulting in a translucent tissue construct (Fig. 7c, ESI Fig. 8†). This result demonstrated that introducing the scaffold to structurally reinforce the hydrogels did not hinder the activities of encapsulated cells.

The use of scaffolds as structural reinforcement would be especially beneficial to supporting weak cell-laden hydrogels. Hydrogels having low crosslinking density are not only structurally weak, but also usually display high swelling properties. Therefore, those hydrogels often result in premature structural disintegration during cell culture, which is facilitated by the cell-induced degradation. In order to demonstrate the scaffold of supporting weak hydrogels, we fabricated the scaffold-reinforced hydrogels encapsulated with fibroblasts using 5 wt% GelMA, which has low elastic modulus (0.3 kPa) and ultimate stress (20 kPa), as shown in Fig. 5. As expected, the pure GelMA hydrogel began to swell extensively, and the overall structure disintegrated during 7 days of culture (Fig. 8a). On the other hand, the swelling and structural disintegration of

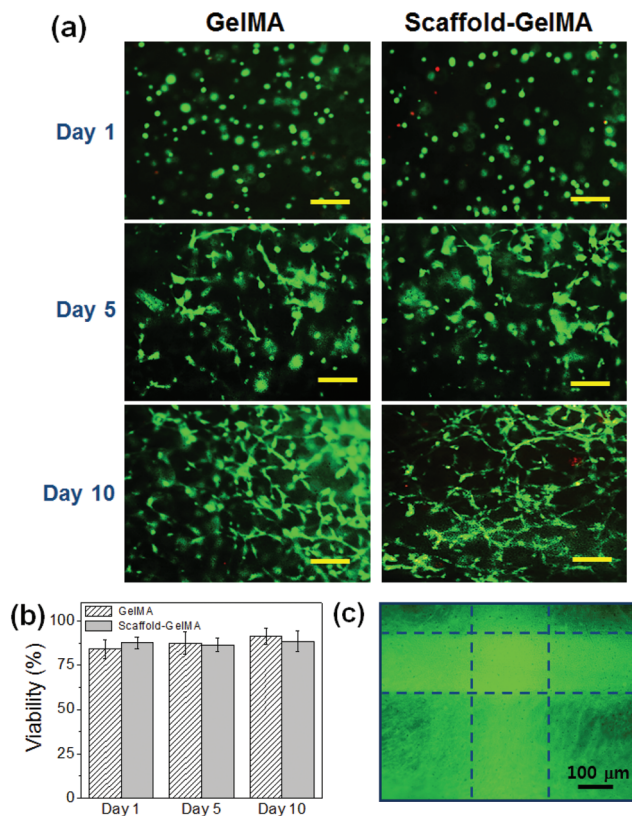


**Fig. 7** (a) Fluorescent microscopic images of GelMA and scaffold-GelMA hydrogels, encapsulated with fibroblasts at days 1, 5 and 10. The cells were stained with calcein-AM (green, live cells) and ethidium homodimer-1 (red, dead cells) (scale bar: 100 μm). (b) The viability of encapsulated fibroblasts in GelMA and scaffold-GelMA hydrogels. (c) Fluorescent microscopic image of fibroblasts within the scaffold-GelMA hydrogel after 21 days of culture. The actin structure of cells was visualized by labeling with Alexa@488-phalloidin. Dotted lines represent the position of the scaffold.

the GelMA hydrogel was prevented by the presence of the scaffold during the same time period (Fig. 8b). This result demonstrated that the PEGDA scaffold could successfully prolong the shape maintenance of weak cell-laden hydrogels.

### 3.5. Effect of scaffold rigidity on encapsulated cells

We further explored the effect of scaffold rigidity on the cells encapsulated within GelMA hydrogels. PEGDA scaffolds with varying rigidity were developed by controlling the concentration of PEGDA used, from 20 to 100 wt%, as shown in Fig. 2c. The viability of fibroblasts encapsulated within GelMA hydrogels (8 wt%) measured over time was not affected by the rigidity of the scaffold; high viability (>80%) was demonstrated under all conditions (ESI Fig. 9†). Interestingly, the cell morphology and proliferation were significantly influenced by the scaffold rigidity; the cells were able to spread and proliferate more quickly within the GelMA hydrogel reinforced with softer scaffolds (Fig. 9). It is well known that fibroblasts are able to sense mechanical signals imparted by their 3D ECM, which in turn allows the cells to exert their force on their surrounding

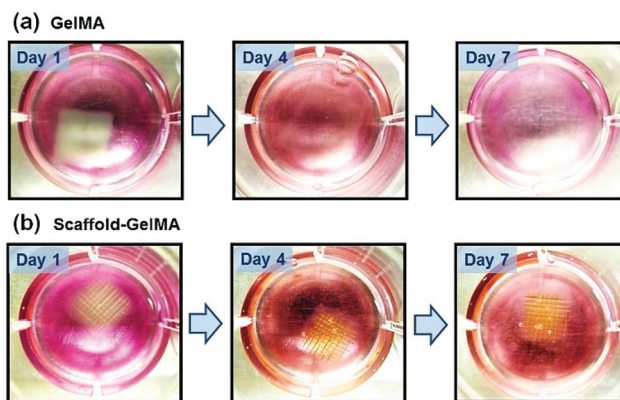


**Fig. 8** Macroscopic views of (a) GelMA hydrogels and (b) scaffold-GelMA hydrogels (5 wt% GelMA) encapsulated with fibroblasts, taken at days 1, 4 and 7 of culture. The GelMA hydrogel without the scaffold disintegrated over time (a), whereas the GelMA hydrogel reinforced with the scaffold was well maintained during the same period (b).

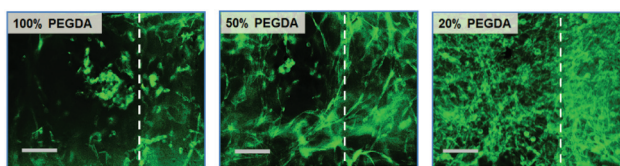


**Fig. 9** Fluorescent images of fibroblasts encapsulated in GelMA hydrogels (8 wt%) supported with PEGDA scaffolds of varying rigidity (100, 50, and 20 wt% PEGDA), taken at day 7 of culture (scale: 100 μm). The cells were stained with Alexa@488-phalloidin to visualize their actin organization. The area right of the dotted line represents the position of the scaffold.

ECM, leading to matrix remodeling, spreading, migration, and proliferation.<sup>37,38</sup> During these events, the overall ECM structure undergoes contraction by the cellular activities. Therefore, it is suggested that the presence of highly rigid scaffolds (*i.e.* 100 wt% PEGDA) may render the hydrogel too stringent, restricting the cells' ability to exert their force and thus subsequent cellular activities, whereas the softer scaffolds allow the hydrogels to be more contractile. It is also possible that the difference in internal tension within the hydrogels, created by the difference in scaffold rigidity, may have influenced differentially the encapsulated cells. Regardless of the scaffold rigidity, the cells within the GelMA hydrogels all demonstrated a high proliferative capacity and resulted in translucent tissue constructs.

## 4. Conclusion

Taken together, we have demonstrated a practical approach to significantly enhance the toughness of cell-laden hydrogels for tissue engineering applications, by introducing a 3D micro-fabricated scaffold designed to act as a structural support. A rapid prototyping technology based on a digital micromirror device projection printing system allowed for efficient fabrica-

tion of 3D scaffolds in microscale dimensions. The scaffold-reinforced hydrogels demonstrated significantly enhanced structural integrity and fracture toughness of the hydrogel without inadvertently affecting the rigidity of the hydrogel, a known regulator of cell behavior. In addition, the biocompatibility of scaffold-reinforced hydrogels was confirmed by evaluating the viability and proliferation of encapsulated cells. Therefore, we expect that the strategy of using 3D scaffolds for hydrogel reinforcement will be highly useful for significantly enhancing the mechanical strength of cell-laden hydrogels for various tissue engineering applications.

## Acknowledgements

The work was supported by funds from the National Science Foundation (CAREER: DMR 0847287), the Presidential Early Career Award for Scientists and Engineers (PECASE), and the National Institutes of Health (HL092836, DE021468, AR05837, EB012597, and HL099073).

## Notes and references

- N. A. Peppas, J. Z. Hilt, A. Khademhosseini and R. Langer, *Adv. Mater.*, 2006, **18**, 1345.
- B. V. Slaughter, S. S. Khurshid, O. Z. Fisher, A. Khademhosseini and N. A. Peppas, *Adv. Mater.*, 2009, **21**, 3307.
- N. Annabi, J. W. Nichol, X. Zhong, C. Ji, S. Koshy, A. Khademhosseini and F. Dehghani, *Tissue Eng. Part B*, 2012, **16**, 371.
- A. S. Hoffman, *Adv. Drug Delivery Rev.*, 2002, **54**, 3.
- C. R. Nuttelman, D. J. Mortisen, S. M. Henry and K. S. Anseth, *J. Biomed. Mater. Res.*, 2001, **57**, 217.
- M. Rafat, F. Li, P. Fagerholm, N. S. Lagali, M. A. Watsky, R. Munger, T. Matsuura and M. Griffith, *Biomaterials*, 2008, **29**, 3960.
- S. Hou, Q. Xu, W. Tian, F. Cui, Q. Cai, J. Ma and I.-S. Lee, *J. Neurosci. Methods*, 2005, **148**, 60.
- D. L. Hern and J. A. Hubbell, *J. Biomed. Mater. Res.*, 1998, **39**, 266.
- F. Yang, C. G. Williams, D.-A. Wang, H. Lee, P. N. Manson and J. Elisseeff, *Biomaterials*, 2005, **26**, 5991.
- U. Hersel, C. Dahmen and H. Kessler, *Biomaterials*, 2003, **24**, 4385.
- K. Y. Lee, J. A. Rowley, P. Eiselt, E. M. Moy, K. H. Bouhadir and D. J. Mooney, *Macromolecules*, 2000, **33**, 4291.
- C. Cha, R. H. Kohman and H. Kong, *Adv. Funct. Mater.*, 2009, **19**, 3056.
- G. D. Prestwich, *Organogenesis*, 2008, **4**, 42.
- B. Bhana, R. K. Iyer, W. L. K. Chen, R. Zhao, K. L. Sider, M. Likhitpanichkul, C. A. Simmons and M. Radisic, *Bio-technol. Bioeng.*, 2010, **105**, 1148.
- A. J. Engler, S. Sen, H. L. Sweeney and D. E. Discher, *Cell*, 2006, **126**, 677.
- J.-Y. Sun, X. Zhao, W. R. K. Illeperuma, O. Chaudhuri, K. H. Oh, D. J. Mooney, J. J. Vlassak and Z. Suo, *Nature*, 2012, **489**, 133.
- H. Shin, B. D. Olsen and A. Khademhosseini, *Biomaterials*, 2012, **33**, 3143.
- P. Schexnaider and G. Schmidt, *Colloid Polym. Sci.*, 2009, **287**, 1.
- A. K. Gaharwar, S. M. Mihaila, A. Swami, A. Patel, S. Sant, R. L. Reis, A. P. Marques, M. E. Gomes and A. Khademhosseini, *Adv. Mater.*, 2013, **25**, 3329.
- E. C. Muniz and G. Geuskens, *Macromolecules*, 2001, **34**, 4480.
- K. Haraguchi and T. Takehisa, *Adv. Mater.*, 2002, **14**, 1120.
- K. Unfried, C. Albrecht, L.-O. Klotz, A. V. Mikecz, S. Grether-Beck and R. P. F. Schins, *Nanotoxicology*, 2007, **1**, 52.
- L. Gilbert, *The Skeletal System*, The Rosen Publishing Group, New York, 2001.
- Y. Lu, G. Mapili, G. Suhali, S. Chen and K. Roy, *J. Biomed. Mater. Res. A*, 2006, **77A**, 396.
- D. Y. Fozdar, P. Soman, J. W. Lee, L.-H. Han and S. Chen, *Adv. Funct. Mater.*, 2011, **21**, 2712.
- P. Soman, J. A. Kelber, J. W. Lee, T. N. Wright, K. S. Vecchio, R. L. Klemke and S. Chen, *Biomaterials*, 2012, **33**, 7064.
- P. Zorlutuna, N. Annabi, G. Camci-Unal, M. Nikkhah, J. M. Cha, J. W. Nichol, A. Manbachi, H. Bae, S. Chen and A. Khademhosseini, *Adv. Mater.*, 2012, **24**, 1782.
- P. Soman, B. D. Tobe, J. Lee, A. M. Winqvist, I. Singec, K. Vecchio, E. Snyder and S. Chen, *Biomed. Microdevices*, 2012, **14**, 829.
- C. Cha, J. H. Jeong, J. Shim and H. Kong, *Acta Biomater.*, 2011, **7**, 3719.
- J. W. Nichol, S. T. Koshy, H. Bae, C. M. Hwang, S. Yamanlar and A. Khademhosseini, *Biomaterials*, 2010, **31**, 5536.
- Y.-C. Chen, R.-Z. Lin, H. Qi, Y. Yang, H. Bae, J. M. Melero-Martin and A. Khademhosseini, *Adv. Funct. Mater.*, 2012, **22**, 2027.
- M. Nikkhah, N. Eshak, P. Zorlutuna, N. Annabi, M. Castello, K. Kim, A. Dolatshahi-Pirouz, F. Edalat, H. Bae, Y. Yang and A. Khademhosseini, *Biomaterials*, 2012, **33**, 9009.
- R.-Z. Lin, Y.-C. Chen, R. Moreno-Luna, A. Khademhosseini and J. M. Melero-Martin, *Biomaterials*, 2013, **34**, 6785.
- M. Kharaziha, M. Nikkhah, S.-R. Shin, N. Annabi, N. Masoumi, A. K. Gaharwar, G. Camci-Unal and A. Khademhosseini, *Biomaterials*, 2013, **34**, 6355.
- C. P. Huang, J. Lu, H. Seon, A. P. Lee, L. A. Flanagan, H.-Y. Kim, A. J. Putnam and N. L. Jeon, *Lab Chip*, 2009, **9**, 1740.
- H. Cho, H.-Y. Kim, J. Y. Kang and T. S. Kim, *J. Colloid Interface Sci.*, 2007, **306**, 379.
- E. Cukierman, R. Pankov and K. M. Yamada, *Curr. Opin. Cell Biol.*, 2002, **14**, 633.
- F. Grinnell, *Trends Cell Biol.*, 2003, **13**, 264.